X-RAY MICROTOMOGRAPHY OF AN ASTM C109 MORTAR EXPOSED TO SULFATE ATTACK

D.P. BENTZ*, NICOS. S. MARTYS*, P. STUTZMAN*, M. S. LEVENSON**, E.J. GARBOCZI*, J. DUNSMUIR+, AND L. M. SCHWARTZ++
* Building and Fire Research Laboratory, Building 226 Room B-350, National Institute of Standards and Technology, Gaithersburg, MD 20899 USA
** Computing and Applied Mathematics Laboratory, Building 101 Room A-337, National Institute of Standards and Technology, Gaithersburg, MD 20899 USA
+ Exxon Research and Engineering Company, Route 22 East, Annandale, NJ 08801 USA
++ Schlumberger-Doll Research, Old Quarry Road, Ridgefield, CT 06877

ABSTRACT

X-ray microtomography can be used to generate three-dimensional 512^3 images of random materials at a resolution of a few micrometers per voxel. This technique has been used to obtain an image of an ASTM C109 mortar sample that had been exposed to a sodium sulfate solution. The three-dimensional image clearly shows sand grains, cement paste, air voids, cracks, and needle-like crystals growing in the air voids. Volume fractions of sand and cement paste determined from the image agree well with the known quantities. Implications for the study of microstructure and proposed uses of X-ray microtomography on cement-based composites are discussed.

INTRODUCTION

The service life and durability of concrete depends on a wide variety of factors [1]. Possible degradation mechanisms include environmental exposure to deleterious compounds of sulfates or chlorides, damage due to frost attack, and spalling as a result of exposure to the high temperature of a fire. The rate of damage can strongly depend on a concrete's transport properties which in turn depend on its microstructure. With knowledge of the three-dimensional concrete microstructure it is possible to determine transport properties that are then used to predict service life. To do this, representative models of the concrete or mortar microstructure are needed.

Two current approaches to representing the microstructure of concrete are 1) constructing ideal models of concrete (e.g., sphere packings modeling the placement of sand in a mortar) and 2) using real two-dimensional images to carry out a variety of studies. For instance, reasonably high resolution two-dimensional images can be made of a mortar or concrete via scanning electron microscopy. Clearly, these two approaches are not mutually exclusive in that data from real images can be used to help guide model building.

In the last decade significant improvements [2] have been made in the development of experimental methods to create three-dimensional images of real microstructures such as sandstone, coal, and biological materials. In particular, it is possible to nondestructively generate maps of X-ray attenuation with about 1 percent accuracy and a resolution of

Mat. Res. Soc. Symp. Proc. Vol. 370 © 1995 Materials Research Society
Materials Research Society. Microstructure of Cement-Based Systems Bonding and Interfaces in Cementitious Materials, Symposia, Novembe 28-December 1, 1994, Boston, MA Diamond, S., Mindess, S., Glasser, P., Roberts, L.W., Skalny, J.P., Wakeley, L.D., Editors, MRS Vol. 3 1995, 1995

about 1 micron [2]. In this paper, we present results of a study concerning the generation of a three-dimensional image of cement mortar using X-ray microtomography. The image processing techniques are discussed. We find that realistic images of the mortar can be made that preserve the volume fractions of cement paste and sand grains.

CEMENT MORTAR SAMPLE PREPARATION

The material studied was an ASTM C109 mortar [3] with a water/cement ratio of 0.485 and a sand/cement ratio of 2.75. The sand grains ranged between 300-600 μm in diameter. Once the sample was made it was cured for 1 day and then exposed to a 10 percent solution of sodium sulfate for about six weeks. To stop further hydration and sulfate attack at a selected testing time the specimen was potted with an ultra-low viscosity resin using a two-step replacement procedure [4]. This procedure also minimizes the occurance of drying shrinkage cracking. First, the pore soultion is replaced with ethanol and then the ethanol is replaced with resin. The resin was cured at 60 degrees centigrade for 24 hours. A cylindrical sample speciman 3.5mm in diameter is then cored from the original mortar to be scanned. Note, tomography does not require the potting procedure, as specimens could be scanned dry or even wet.

X-RAY MICROTOMOGRAPHY

The three-dimensional x-ray attenuation map of the cement mortar was generated at the National Synchrotron Light Source (NSLS) located at Brookhaven National Laboratory using Exxon's microtomography scanner at beamline X-2B. This instrument is an optical microscope that images scintillation events in a phosphor onto the surface of a 512x512 cooled CCD. X-rays illuminate a cylindrical specimen and radiographic images are acquired at a large number of discrete view angles as the specimen is rotated about its axis. This rotation axis is perpendicular to the x-ray beam and parallel to the CCD pixel columns. At the conclusion of a scan the image data from the CCD are sorted such that the specimen projections for each pixel row are collected together. These collected data are reconstructed to form a single 2-D tomographic slice. Since the synchrotron beam is highly collimated, a fast Direct Fourier inversion algorithm is used to rapidly reconstruct the 512 slices corresponding to each CCD row. Three dimensional volumes are built up by stacking the slices. Beam hardening artifacts are eliminated by using a Silicon monochromator to select a well defined energy.

Under ideal conditions the ultimate spatial resolution of this instrument is comparable to a light microscope and is about 1 micron. For this study the spatial resolution is limited by the specimen size which is about 3.5mm. With a field of view for the mortar specimen of slightly greater than 3.5mm, each pixel represents about 7 microns.

The mortar specimen in this study was scanned at 17 keV and radiographic images were acquired in 0.36 degree increments between 0 and 180 degrees of specimen rotation. Data acquisition and reconstruction were completed in 1.5 hours. This scanning protocol resulted in a reconstructed volume that is more noisy than what is usually achieveable. The protocol for future scans will be modified to reduce noise.

RESULTS-IMAGE PROCESSING TECHNIQUES

Figure 1 is a two-dimensional image of the attenuation coefficients of a plane from the reconstruction of the X-ray tomography data. Note that there are a wide variety of features present in the image. The light areas represent cement paste, the somewhat darker areas are sand grains and the darkest areas are air voids. Inside the air voids are crystalline growths, which most likely are calcium hydroxide or possibly gypsum or ettringite. There is also a crack resulting from the sulfate attack. Notice also the existence of concentric rings, which are an artifact of the tomographical data collection process. Also, there is some noise which may, in part, be due to the local inhomogeneity of the component materials.

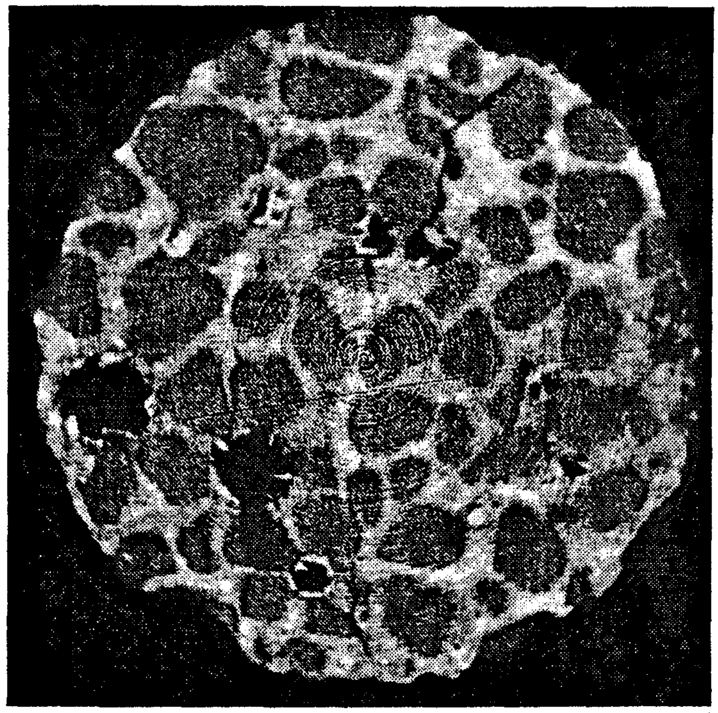

Figure 1: Original two-dimensional image obtained from tomography data set.

For this preliminary study we decided to subdivide the image into three separate phases: sand, cement paste and air voids. Although there are many other features, as described above, these three phases make the largest volumetric contribution and are clearly (at least to the eye) distinguishable.

Once the decision is made to convert the original attenuation coefficients into three phases, a procedure must be developed to decide what voxel (volume element) corresponds to what phase. Due to the noise present in the original image it is not easy to systematically separate the phases. For instance a simple thresholding of the attenuation coefficients, which range in value over two decades, produces an unrealistic image.

In order to produce a more realistic image, a four step image processing procedure was performed. The first step was intended to remove the ringing artifact and some of the local variation from the image. We chose a technique based on the discrete wavelet transform [5]. In many ways the wavelet transform is similar to the Fourier transform. It consists of representing the image as a weighted sum of basis elements. With the Fourier transform, the basis elements are the *sine* and *cosine* functions of different frequencies. The wavelet basis elements also have different frequencies. However, unlike the Fourier transform, a wavelet basis element is nonzero only in a finite region. Therefore, high frequency noise can be removed locally instead of globally as in the case of the Fourier transform. As a result, an advantage of the wavelet transform over the Fourier transform is that it is capable of preserving boundaries better. The particular wavelet technique employed is based on the thresholding idea of Donoho [6].

In figure 2 we show a comparison of attenuation profiles before and after the wavelet processing.

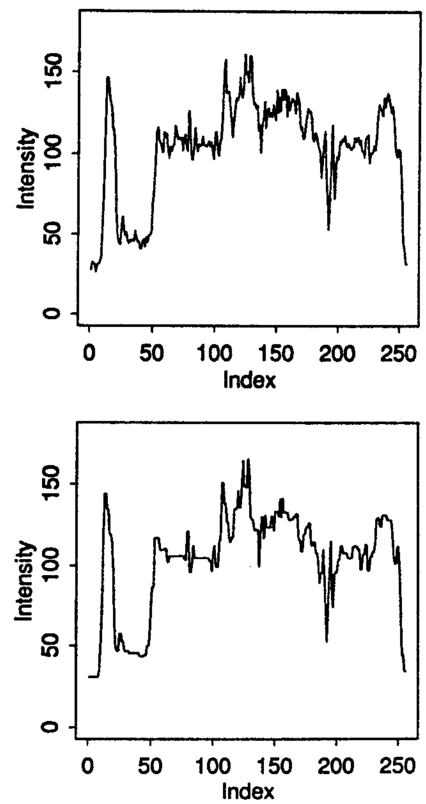

Figure 2: Attenuation profiles of figure 1 along a vertical line before (top) and after (bottom) wavelet filtering.

Clearly plateaus are beginning to form that correspond to the different phases. Also the boundaries are generally preserved. For instance the rapid fluctuation of attenuation coefficients around voxels 190 to 200 has not been diminished. This fluctuation corresponds to the two small air voids in the original image.

Next thresholding was preformed on the image to segment it into the three phases. We found there was still some spurious noise which was cleared up with use of a median filter [7].

The final stage removed the unphysical presence of a band of sand surrounding air voids. This is due to the interpolation of the attenuation coefficient in regions where air voids border the cement paste. To remove the bordering of spurious sand, the regions near the sand-air void boundary were dilated (i.e., sand regions neighboring air-void were converted to air-void). Figure 3 shows the final processed image.

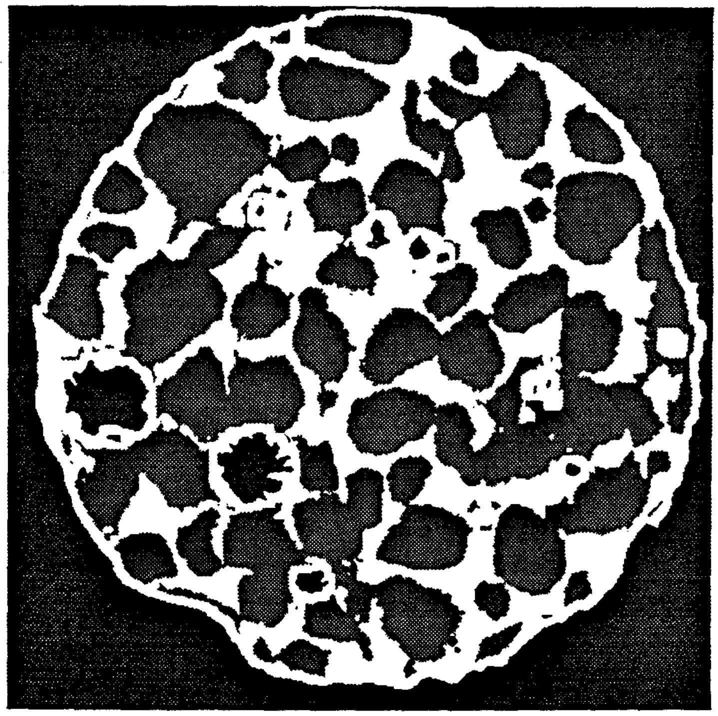

Figure 3: Final processed image. Black corresponds to air voids, grey to sand and white to cement paste.

Once all the images had been processed, we then determined the ratio of sand to cement in the three demensional reconstruction of the mortar and found it was in excellent agreement with the mix design (i.e., 55 volume percent sand, 45 volume percent paste). We are currently studying the sand grain size distribution. Here, there is the difficulty that one must carefully separate touching sand grains. However, our preliminary studies, employing watershed segmentation techniques [8] are encouraging.

CONCLUSIONS-FUTURE RESEARCH

The use of X-ray microtomography to investigate the three-dimensional microstructure of a cement mortar has been demonstrated. For our study, resolution of order 10 μm was sufficient to visualize the main features of a mortar. At higher resolutions other features in the mortar, such as the interfacial zone microstructure at the sand grain/cement paste may become more apparent. Limits to the size of sample studied depends on the resolution needed. Since the CCD used in the data collection had 512 pixels accross, the resolution is W/512 where W is the sample width. Studying larger samples will therefore sacrifice resolution.

Future research includes the studying the size and spacing between sand grains or air voids, the ingress of materials into mortar, the interfacial zone, the flocculation structure of cement grains, fracture, and computation of stress fields and elastic moduli. With realistic three-dimensional images of mortar available it should be possible to better understand transport properties and degradation processes in mortars and concrete.

REFERENCES

[1] J. M. Scanlon, editor, Concrete Durability, American Concrete Institute, P.O. Box 19150, Redford Station, Detroit, MI 48219 (1987).

[2] B.P. Flannery, H. W. Deckman, W. G. Roberge, and K. L. D'Amico, Science, 235, 1439 (1987).

[3] ASTM C109 Standard Test Method for Compressize Strength of Hydraulic Cement Mortar, 1993 Annual Book of ASTM Standards, ASTM, 1916 Race Steet, Philadelphia, PA 19103.

[4] L. J. Struble and P. E. Stutzman, J. Mat. Sci. Let., 8, 632 (1989).

[5] I. Daubechies, Wavelets, SIAM, Philadelphia PA (1992).

[6] D. Donoho, Nonlinear wavelet methods for recovery of signal, densities, and spectra from indirect and noisy data , available through ftp at playfair.stanford.edu.

[7] V. Cantoni, S. Levialdi, and G. Musso, Editors, Image analysis and Processing, (Plenum Press, New York 1986).

[8] J. C. Russ and J. C. Russ, Acta Sterologica, 7(1), 33-4, (1988).